ACS APPLIED MATERIALS & INTERFACES

Research Article

www.acsami.org

Confined Catalysis in the g-C_3N_4/Pt(111) Interface: Feasible Molecule Intercalation, Tunable Molecule–Metal Interaction, and Enhanced Reaction Activity of CO Oxidation

Shujiao Wang, Yingxin Feng, Ming'an Yu, Qiang Wan, and Sen Lin*

State Key Laboratory of Photocatalysis on Energy and Environment, College of Chemistry, Fuzhou University, Fuzhou 350002, China

S upport n In or at on

ABSTRACT: The deposition of a two-dimensional (2D) atomic nanosheet on a metal surface has been considered as a new route for tuning the molecule–metal interaction and surface reactivity in terms of the confinement effect. In this work, we use first-principles calculations to systematically explore a novel nanospace constructed by placing a 2D graphitic carbon nitride (g-C_3N_4) nanosheet over a Pt(111) surface. The confined catalytic activity in this nanospace is investigated using CO oxidation as a model reaction. With the inherent triangular pores in the g-C_3N_4 overlayer being taken advantage of, molecules such as CO and O_2 can diffuse to adsorb on the Pt(111) surface underneath the g-C_3N_4 overlayer. Moreover, the mechanism of intercalation is also elucidated, and the results reveal that the energy barrier depends mainly on the properties of the molecule and the channel. Importantly, the molecule–catalyst interaction can be tuned by the g-C_3N_4 overlayer, considerably reducing the adsorption energy of CO on Pt(111) and leading to enhanced reactivity in CO oxidation. This work will provide important insight for constructing a promising nanoreactor in which the following is observed: The molecule intercalation is facile; the molecule–metal interaction is efficiently tuned; the metal-catalyzed reaction is promoted.

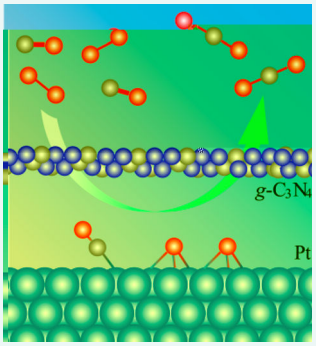

KEYWORDS: *confinement effect, molecule intercalation, CO oxidation, g-C_3N_4, Pt(111), first-principles*

Downloaded via FUZHOU UNIV on September 15, 2018 at 06:28:25 (UTC).
See https://pubs.acs.org/sharingguidelines for options on how to legitimately share published articles.

1. INTRODUCTION

Transition metals are well-known heterogeneous catalysts and have been widely investigated in the past few years.[1−4] For the design of more efficient transition-metal catalysts, great efforts have been made to tune molecule–catalyst interactions.[5] Recent experimental studies suggest that the reactivity of transition-metal surfaces can be promoted by placing a two-dimensional (2D) material over the metal surface.[5−17] For example, Bao and co-workers found that the confinement effect of a h-BN or graphene cover results in the considerably reduced adsorption energy of CO and the promoted reactivity of CO oxidation at the 2D/metal interface.[6,18] Ferrighi et al. elucidated the reactivity of O_2 and H_2O at the interface between graphene and the TiO_2 surface and indicated the importance of the confinement effect in photocatalysis.[19]

While the placement of a 2D cover over the metal surface is becoming a popular route to tune the molecule–catalyst interaction, very little is known about the mechanism, including how the molecules intercalate into the 2D/metal interface and how the cover tunes the molecule–metal interaction. In fact, most of the reported covers such as graphene[6] and h-BN[12,18] have no inherent channels, and it is difficult for the molecules to intercalate into the 2D/metal interface unless defects including islands, domain boundaries, and wrinkles are available. As reported by Bao et al., upon CO exposure (5.0×10^{-8} Torr) at room temperature, the Pt(111) surface under h-BN islands becomes covered by the rapid adsorption of CO.[18] By contrast, under similar CO exposure conditions, no CO intercalation was observed on the full h-BN layer without any defects. A similar phenomenon was also observed in the molecular intercalation of graphene. Therefore, it is supposed that the defects in the covers play an important role in the molecular intercalation.[5,6,17,18] Unfortunately, the formation of these defects often depends on the synthesis conditions, making the defects not uniform. Therefore, the search for a new 2D nanomaterial that can provide uniform channels for molecular intercalation remains a challenge in the design and synthesis of confined catalysts.

Among the 2D materials, graphitic carbon nitride (g-C_3N_4), a newly emerged material, exhibits high chemical stability and an appealing electronic structure, being a wide-bandgap semiconductor.[20−25] This allows its direct use as a semiconductor photocatalyst in the direct splitting of water into hydrogen and oxygen. Unlike graphene and h-BN, g-C_3N_4 has inherent triangular pores formed by six edge nitrogen atoms. Given such a unique porous structure of g-C_3N_4, it is natural to ask whether these pores can be adopted as channels for the intercalation of gas molecules onto the metal surface covered by g-C_3N_4. To the best of our knowledge, there are few reports about the confined catalysis on transition-metal surfaces covered by porous materials.

Received: June 16, 2017
Accepted: September 6, 2017
Published: September 6, 2017

© 2017 American Chemical Society

DOI: 10.1021/acsami.7b08665
ACS Appl. Mater. Interfaces 2017, 9, 33267−33273

In this work, a g-C_3N_4/Pt(111) system is proposed and investigated using density functional theory (DFT) calculations. The confined catalysis of CO oxidation is used as a test case. Our calculation results reveal that CO and O_2 molecules can intercalate through the triangular pores of g-C_3N_4 to adsorb on Pt(111). The molecule−catalyst interaction is successfully tuned by the g-C_3N_4 cover resulting in a decreased binding energy of CO on Pt(111). In addition, for a better understanding of the confined catalysis, a detailed reaction mechanism of CO oxidation is also proposed. These findings provide important insight for designing promising nanospaces for confined catalysis with high performance. This publication is organized as follows. The calculation details are described in Section 2. The results and discussion are presented in Section 3. The conclusions are given in Section 4.

2. COMPUTATIONAL DETAILS

All calculations were carried out by using the Vienna *ab initio* simulation package (VASP) within the generalized gradient approximation (GGA)[26−28] using the PBE (Perdew−Burke−Ernzerhof) exchange-correlation functional. For an accurate description of the van der Waals interactions between g-C_3N_4 and Pt(111), the van der Waals density functional (vdW-DF) method of Dion et al. was adopted, and the optPBE-vdW functional was employed in this work, as this optimized functional has yielded excellent results in previously reported studies.[29−31] The electronic wave functions were expanded in plane waves up to a cutoff energy of 400 eV, and the ionic core electrons were approximated by the projector augmented-wave (PAW) method.[32] The calculated g-C_3N_4 lattice parameter of 7.34 Å is consistent with the experimental (7.30 Å) value[33] and other theoretical results.[33−36] The periodicity of the g-C_3N_4/Pt(111) system can be successfully achieved by using a three-layer slab containing a $\sqrt{7} \times \sqrt{7}$ unit cell of Pt(111) covered by a 3 × 3 unit cell of g-C_3N_4. For the structural optimizations, the atoms in the bottom metal layer were fixed while the other atoms including adsorbates were fully relaxed. For avoidance of the artificial interactions along the z-direction between the slab and its repeated images, a vacuum space with a length of about 14 Å was employed. A 2 × 2 × 1 Monkhorst−Pack k-point grid[37] was adopted to sample the Brillouin zone.[38−40] The electron density for the ground states was converged with a 10^{-4} eV total energy threshold, and the geometries were optimized until the maximum force on any ion was less than 0.05 eV/Å.

For the adsorption energy E_{ads}, it was defined by $E_{ads} = E_{(adsorbate+catalyst)} - E_{(free\text{-}molecule\text{-}or\text{-}atom)} - E_{(free\text{-}catalyst)}$ in which the terms are as follows: $E_{(adsorbate+catalyst)}$ is the total energy of the system; $E_{(free\text{-}molecule\text{-}or\text{-}atom)}$ is the energy of free molecule or atom adsorption; $E_{(free\text{-}catalyst)}$ is the total energy of a free catalyst. More negative E_{ads} indicates an energetically more favorable process.

The nudged elastic band (NEB)[41−43] approach was adopted to simulate CO oxidation, generating the minimum energy path of the reaction process and an evaluation of the energy barrier on the potential energy surface. The activation barrier E_a for each reaction step was calculated by the energy difference between the transition state (TS) and initial state (IS) while the reaction energy ΔE for each reaction step was calculated by the energy difference between the final state (FS) and the initial state.

3. RESULTS AND DISCUSSION

3.1. g-C_3N_4/Pt(111) Interface Model. As reported by experimental studies, g-C_3N_4 has a 2D planar structure that is quite similar to that of graphene and h-BN. As shown in Figure 1, g-C_3N_4 consists of heptazine units, in which each carbon

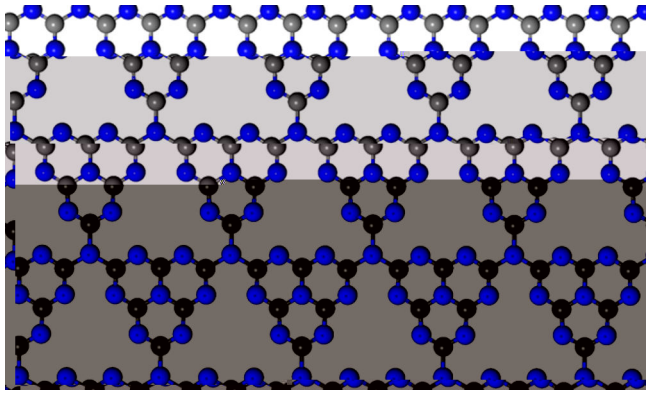

Figure 1. Optimized structure of g-C_3N_4. Color scheme: C, gray; N, blue.

atom is connected to three nitrogen atoms. The bridge N atoms and inner N atoms are all 3-fold coordinated by three C atoms while the edge N atoms are 2-fold coordinated by two C atoms, generating a particular porous structure.

The optimized g-C_3N_4/Pt(111) configuration is displayed in Figure 2. It is clear that the g-C_3N_4 plane is somewhat distorted after being placed on Pt(111) and that the distance ($d_{nanospace}$) between g-C_3N_4 and Pt(111) is calculated to be 3.66 Å, which is comparable to those of h-BN (3.16 Å)[18] and graphene (3.30 Å)[6] on metal surfaces. Different from the cases of graphene and h-BN supported by metal surfaces, there are two Pt surface regions with one fully covered by the heptazine units of g-C_3N_4 and another under the triangular pores. Accordingly, the possible adsorption sites on the Pt(111) surface covered by g-C_3N_4 are indicated as top, fcc, and hcp for the former and pore-top, pore-fcc, and pore-hcp for the latter.

3.2. Adsorption of CO, O_2, O, and CO_2. To explore how the g-C_3N_4 cover tunes the molecule−metal interaction and achieve a fundamental insight into the catalytic performance of the Pt(111) covered by the g-C_3N_4 monolayer, CO oxidation is selected as a model reaction, and a systematic understanding of the adsorption behavior of involved species, including reactants, intermediates, and products, is provided. The preferred adsorption sites and energies of CO, O_2, O, and CO_2 are listed in Table 1, and the corresponding adsorption patterns are displayed in Figure 3. The detailed information for all adsorption states can be seen in Table S1 in the Supporting Information (SI). It is clear that the adsorption of all species with the exception of atomic oxygen are weaker at the g-C_3N_4/Pt(111) interface than on the pure Pt(111) surface, revealing the crucial role that g-C_3N_4 plays in tuning the molecule−metal interaction.

CO. As shown in Figure 3a, CO adsorbs at the fcc site of Pt(111) under the g-C_3N_4 cover with the adsorption energy of −1.40 eV, which is approximately 0.44 eV larger than that on the pure Pt(111) surface. The three Pt−C bond lengths are calculated to be 2.12, 2.12, and 2.11 Å, and the C−O bond is approximately 1.20 Å, slightly longer than that without the g-C_3N_4 cover. At the hcp site, the adsorption energy is slightly higher. For these two adsorption states, the height of the

DOI: 10.1021/acsami.7b08665
ACS Appl. Mater. Interfaces 2017, 9, 33267−33273

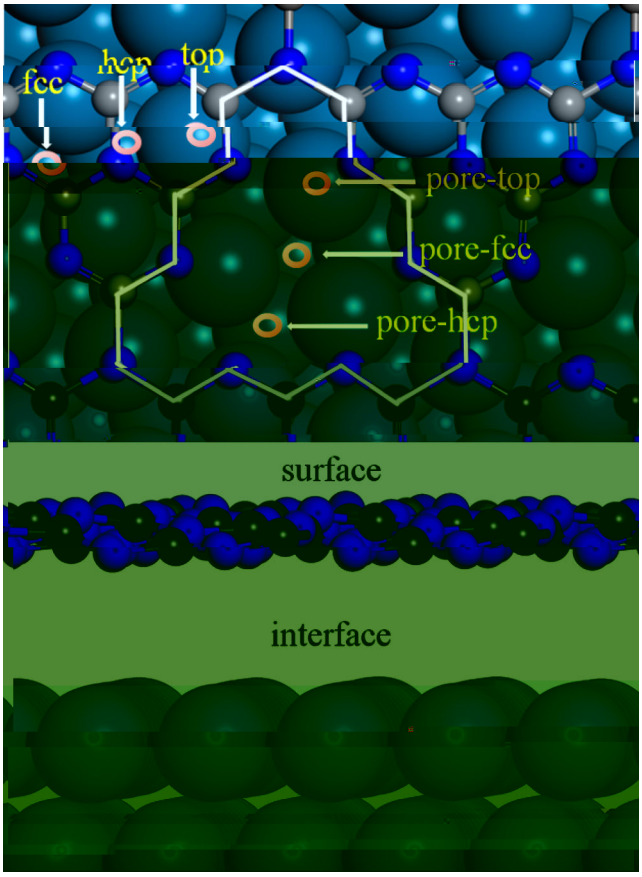

Figure 2. Top and side view of the optimized structure of g-C_3N_4/Pt(111) with possible adsorption sites. Color scheme: C, gray; N, blue; Pt, indigo.

Table 1. Calculated Adsorption Energies of CO, O_2, O, and CO_2 on the Pt(111) Surface with and without the g-C_3N_4 Cover

	adsorption energy (eV)	
species	without cover	with cover
CO	−1.84	−1.40
O_2	−0.93	−0.75
O	−1.39	−1.41
CO_2	−0.48	0.38

nanospace is approximately 5.23 Å, which is much larger than that before the molecules' adsorption. While the CO molecule is located on the top of the Pt atom, the binding energy is considerably reduced by 0.61 eV under the cover, and the average $d_{nanospace}$ is increased to 5.52 Å. Furthermore, we also investigate the adsorption behavior of CO under the triangular pores, and it can be seen from Table S1 that the adsorption energies are decreased with the calculated values close to those for the sites under the heptazine units. Similar results were obtained for h-BN/Pt(111) and graphene/Pt(111) interfaces where the adsorption energies of CO were reduced by 0.51[6] and 0.42 eV,[18] respectively. It appears that g-C_3N_4 may be a more promising cover that can more greatly tune the molecule−metal interaction.

To further understand how the g-C_3N_4 cover tunes the interaction between CO and Pt(111), we calculated the differential charge density of CO adsorbed at the g-C_3N_4/Pt(111) interface which is plotted in Figure 4. Considerable

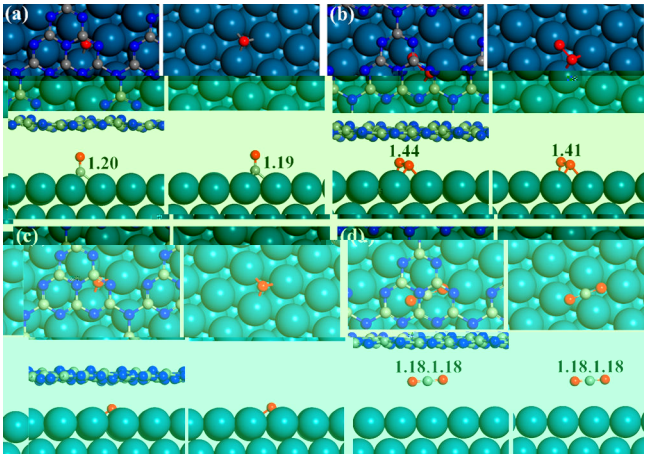

Figure 3. Optimized structures of CO (a), O_2 (b), O (c), and CO_2 (d) adsorption on the Pt(111) surface with (left) and without (right) the g-C_3N_4 cover. Color scheme: C, gray; N, blue; O, red; Pt, indigo.

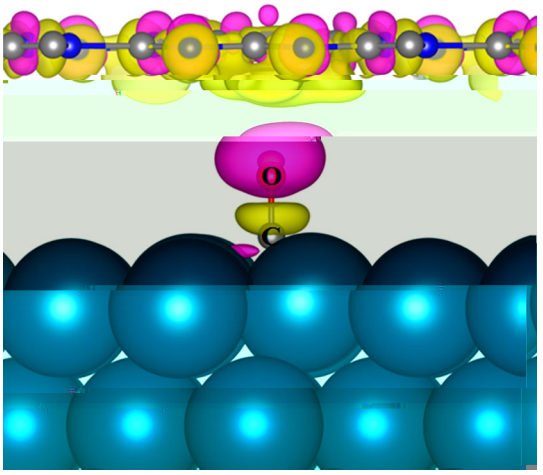

Figure 4. Calculated differential charge density of CO adsorbed at the g-C_3N_4/Pt(111) interface. Yellow and purple represent charge depletion and accumulation, respectively. The isovalue is ±0.0006 au. Color scheme: C, gray; N, blue; O, red; Pt, indigo.

electron transfer from the g-C_3N_4 cover to the CO species is observed. Obviously, the g-C_3N_4 cover and CO species become positively and negatively charged, respectively. This may generate an attraction between g-C_3N_4 and CO, thus reducing the binding energy of CO on Pt(111). Furthermore, we also find that the electronic interaction between g-C_3N_4 and CO leads to a charge depletion in the bond between C and O, which is consistent with the fact that CO bond length is slightly elongated by 0.01 Å. According to Bader charge calculation[44] results, the charge transfer from Pt(111) to CO is approximately 0.17 |e| while, under the g-C_3N_4 cover, this value decreases to only 0.11 |e|, revealing a weakened interaction between CO and Pt(111). This may have contributed to the fact that g-C_3N_4 provides extra charge (0.14 |e|) to CO. These results suggest that the g-C_3N_4 overlayer can weaken the strong interaction between CO and Pt.

O_2. As shown in Figure 3b, the adsorption of O_2 on both the g-C_3N_4/Pt(111) and pure Pt(111) is investigated. The O_2 molecule is found to lie at the fcc site of pure Pt(111) with the binding energy of −0.93 eV. Similar to that in the case of CO,

DOI: 10.1021/acsami.7b08665
ACS Appl. Mater. Interfaces 2017, 9, 33267−33273

this value is also increased by approximately 0.20 eV after the *g*-C_3N_4 cover is added, and the calculated O−O bond length is changed from 1.41 to 1.44 Å, revealing an obvious confinement effect in O_2 adsorption. Differently from the perpendicular adsorption of CO, the calculated $d_{nanospace}$ is approximately 4.13 Å which is slightly larger than that before adsorption.

O. As a dissociative product of the O_2 molecule, the oxygen atom prefers to adsorb at the fcc site (as shown in Figure 3c) on the Pt(111) surface. At the interface, the calculated O−Pt bond lengths are 2.05, 2.05, and 2.05 Å, and the $d_{nanospace}$ is approximately 4.65 Å. The adsorption energies are almost equal to the values of −1.41 and −1.39 eV before and after the addition of the *g*-C_3N_4 cover over Pt(111), suggesting that the *g*-C_3N_4 cover does not affect the adsorption of the oxygen atom on the Pt(111) surface. This phenomenon is further confirmed by the Bader charge calculations showing that no charge transfer occurs from the *g*-C_3N_4 cover to the atomic O connected to the Pt atoms.

CO_2. As displayed in Figure 3d, CO_2 adsorbed on the Pt(111) surface as a linear molecule. This state has the positive binding energy of 0.38 eV, suggesting that the attraction interaction between CO_2 and the Pt surface is so weak that spontaneous adsorption of CO_2 will not occur on the Pt(111) underneath the *g*-C_3N_4 cover. By contrast, on the pure Pt(111) surface, the calculated binding energy of −0.48 eV is found, indicating that the cover effect is also important for CO_2 adsorption. Another adsorption state of CO_2 is also detected in this work with a bent configuration, for which the binding energy is more positive with the value of 0.45 eV with the C and O atoms connecting to surface Pt atoms. We believe that such an unstable adsorption will help the CO_2 generated from CO oxidation to facilely escape from the catalyst.

3.3. Intercalation of CO and O2 at the *g*-C3N4/Pt(111) Interface. Before exploration of the CO oxidation reaction, there is an important issue that remains to be resolved, that is, how the reactants CO and O_2 intercalate into the *g*-C_3N_4/Pt(111) interface. As reported by previous experimental studies, graphene[6] or *h*-BN[12] has no inherent channels, and defects are constructed for the intercalation of the molecules. However, the intercalation mechanism is still not fully understood. Here, using the triangular pores of *g*-C_3N_4 as channels, the mechanism for the CO and O_2 intercalating into the *g*-C_3N_4/Pt(111) interface as well as the diffusion of CO_2 out of the interface is studied systematically.

The diagrams of IS, TS, and FS of O_2, CO, and CO_2 intercalation at the *g*-C_3N_4/Pt(111) interface are displayed in Figure 5. In the initial state, O_2 is physically adsorbed over the *g*-C_3N_4 surface. The transition state prefers the configuration where both O atoms are located at the two sides of the *g*-C_3N_4 layer (Figure 5a). The O−O bond length is compressed to 1.23 Å, and the calculated distances between the O atoms and the edge nitrogen atoms are approximately 2.52 Å. The calculated $d_{nanospace}$ is approximately 3.57 Å, slightly shorter than that in the initial state. An energy barrier of 0.83 eV is required for this process, and the reaction is highly exothermic (−1.50 eV). A similar barrier of 0.69 eV is found for the N_2 molecule passing through the pore of *g*-C_3N_3 with the large pore diameter of 5.46 Å.[45] According to the Bader charge calculations, the charges carried by the O atoms are 0 |*e*| because O_2 is a nonpolar binary molecule, and the edge N atoms in the pores are negatively charged. When O_2 passes through the pore, the interaction between O_2 and edge N atoms is weak.

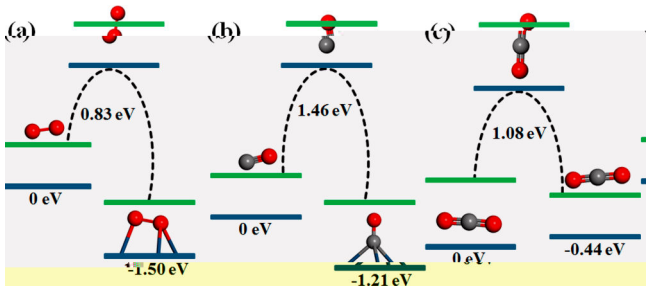

Figure 5. Diagrams of initial state (IS), transition state (TS), and final state (FS) with relative energies of O_2 (a), CO (b), and CO_2 (c) intercalation at the *g*-C_3N_4/Pt(111) interface. To be clear, the green and blue bars are used to represent *g*-C_3N_4 and Pt(111), respectively. Color scheme: C, gray; O, red. Optimized geometries can be seen in Figure S1.

For CO intercalation, a higher barrier of 1.46 eV should be overcome for passing through the interface to adsorb on Pt(111). In the transition state, the O atom of CO is located in the cover plane with the C atom totally under the cover, and the $d_{nanospace}$ value is changed from 3.54 to 3.91 Å. Unlike O_2, CO is a polar molecule with the C and O atoms possessing 1.12 and −1.12 |*e*| charge, respectively. Considering the negatively charged N atoms, it is more difficult for the O atom of CO to diffuse than for the C atom because of its repulsive interaction with N atoms. Therefore, this process requires a higher energy barrier than that for O_2. Interestingly, when an oxygen atom is preadsorbed on Pt(111) (as shown in Figure S2), the energy barrier for O_2 intercalation is reduced to 1.31 eV, indicating that preadsorbed species on a metal surface can help the intercalation of molecules.

Finally, we investigate the diffusion of CO_2 out of the *g*-C_3N_4/Pt(111) interface. On the basis of the calculation results, CO_2 should overcome the energy barrier of 1.08 eV to pass through the pore in the *g*-C_3N_4 layer from Pt(111). In the TS, one O atom and C atom of CO_2 are located at one side with another O atom barely in the *g*-C_3N_4 plane. The Bader charge calculation results indicate that, in this state, the C atom carries +2.11 |*e*|, and each O atom possesses about −1.05 |*e*|. Similar to that for CO, a repulsive interaction will also be generated because of the negatively charged edge N atoms, thus leading to a high energy barrier for intercalation. For the reverse process, namely, the intercalation of CO_2 at the interface, it is necessary to overcome the energy barrier of 1.52 eV, larger than that for CO, which may be due to the larger size of CO_2.

On the basis of the above results, it can be concluded that there are two factors that can control the intercalation of a molecule at the *g*-C_3N_4/Pt(111) interface. The first is the property of the molecule, and the other is the property of the channel. The former mainly includes the size and charge characteristics of the molecule. For the latter, the pore size (steric effect) and the charge characteristics of the atoms along the pores are the primary crucial factors. By contrast, for the other reported covers such as *h*-BN and graphene which have no inherent channels, the molecules should pass through the defects including islands, domain boundaries, and wrinkles.[18,46,47] In these cases, the molecules interact directly with both the metal surface and the cover. In such a process, the cover will be lifted up, requiring extra energy.

3.4. CO Oxidation at the *g*-C_3N_4/Pt(111) Interface. Given that small molecules can diffuse through the *g*-C_3N_4 cover to adsorb on the Pt(111) surface, the interface between *g*-

DOI: 10.1021/acsami.7b08665
ACS Appl. Mater. Interfaces 2017, 9, 33267−33273

C_3N_4 and Pt(111) can be considered as a 2D nanoreactor for certain reactions. CO oxidation was investigated as a model reaction for this purpose. For comparison, the catalytic reaction over a bare Pt(111) surface was also studied.

From the above section, it is believed that O_2 can intercalate at the interface before the CO species because of a lower energy barrier. As shown in Figure 6a, O_2 is found to dissociate to two

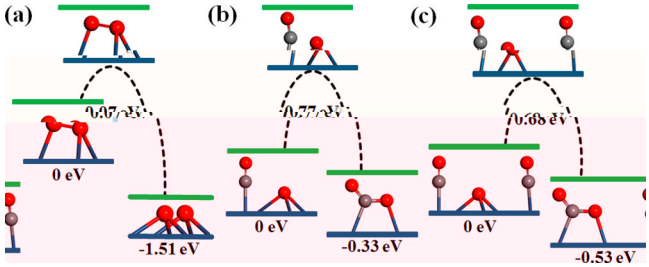

Figure 6. Diagrams of IS, TS, and FS with relative energies for O_2 dissociation (a) and CO oxidation (b, c) at the g-C_3N_4/Pt(111) interface. The green and blue bars are used to represent g-C_3N_4 and

atomic O species with the energy barrier as low as 0.07 eV and the exothermicity of about −1.51 eV, indicating that this can be a facile process at low temperature. In the transition state, the O−O bond length is elongated to 1.42 from 1.40 Å in the initial state. After the reaction, two O atoms are observed at the fcc sites. On the bare Pt(111) surface, the O−O distance in the TS is approximately 1.42 Å, and the calculation results show that this reaction must overcome a higher energy barrier of approximately 0.33 eV and that the exothermicity is −1.39 eV as shown in Figure S3a. Obviously, the cover effect indeed plays an important role in promoting the reaction activity of oxygen dissociation. For a better understanding of the role that the g-C_3N_4 cover plays in the reaction, differential charge density of the TS for O_2 dissociation is also calculated in this work. Considerable electron transfer from the g-C_3N_4 cover to O−O species and accumulation in the O−O bond region can be observed in Figure 7a. The excess electron may fill the $2\pi^*$ orbital of O_2 species and make it easier for the O−O bond to be broken.

Once the CO intercalates at the interface with available active oxygen atoms, we can examine how it reacts with O to produce CO_2. Examination of Figure 6b shows that, underneath the g-C_3N_4 cover, the energy barrier for the CO + O → CO_2 reaction following the Langmuir−Hinshelwood mechanism is approximately 0.77 eV, which is lower than that (0.85 eV) on pure Pt(111). Furthermore, the reaction is found to be more exothermic underneath the cover. In the IS, CO and O are coadsorbed at the top and fcc sites, respectively, with the C−O distance being 1.16 Å. In the TS, the O−C−O angle is approximately 108.88°. Similar to that (as shown in Figure S3b) on Pt(111), after the reaction, a bent CO_2 is generated with C and O connecting to two Pt surface atoms. Optimized geometries of the IS, TS, and FS are shown in Figure S4. The binding energy of this product is approximately 0.45 eV, indicating that it is not stable at the interface and may diffuse out of the nanospace through triangular pores. These findings reveal that CO oxidation at the g-C_3N_4/Pt(111) interface can be enhanced because of the considerably reduced binding energy of CO by the confinement effect. Figure 7b shows that, on the one hand, the electron density is depleted at the nitrogen atom of the g-C_3N_4 cover just above the adsorbed CO species and in the C−O bond of CO, indicating that the original C−O bond is now weakened. On the other hand, considerable electron density is found to accumulate between the O atom near its CO species and the carbon atom, promoting the formation of the new C−O bond.

In addition, CO oxidation in the presence of an adsorbed CO on Pt(111) is studied. As shown in Figure 6c, in the initial state, a CO molecule is adsorbed near the coadsorbed CO and O. The calculated $d_{\text{nanospace}}$ is approximately 5.80 Å, larger than that (5.49 Å) without the preadsorbed CO species. Interestingly, the energy barrier is approximately 0.10 eV lower, and the reaction becomes more exothermic (−0.53 eV). Obviously, there is always energy consumed to lift the g-C_3N_4 cover during the CO oxidation. Our results clearly reveal that the perpendicularly preadsorbed CO species help lift the g-C_3N_4 cover slightly, making the attack of CO to O more facile. Similar charge distribution at the TS of CO oxidation can be observed in Figure S5.

Therefore, it is believed that the g-C_3N_4 cover can provide excess electron density to weaken the original C−O bond and promote the formation of the new C−O bond, thus reducing the reaction energy barrier for CO oxidation.

4. CONCLUSIONS

In this current work, the g-C_3N_4/Pt(111) interface is studied by using a DFT method in an effort to gain insight into the molecule intercalation, the tuning of the molecule−metal interaction, and the reaction activity of CO oxidation under the confinement effect. From the calculation results, we find that the intercalation of molecules through the inherent pores of g-C_3N_4 onto Pt(111) was feasible, and the intercalation energy barrier mainly depends on the properties of the molecule. The interaction between CO and Pt(111) is significantly weak because of the charge transfer from the g-C_3N_4 cover to CO species. The O_2 molecule is found to facilely dissociate on the g-C_3N_4/Pt(111) interface, producing an active oxygen atom for relevant reactions. The energy barrier for CO oxidation in the g-C_3N_4/Pt(111) interface is reduced when compared with that on pure Pt(111), suggesting a promoted reaction activity under the confinement effect. This work confirms that the g-C_3N_4 can provide uniform channels for the molecule intercalation and can be used as a promoter to tune the molecule−metal interaction and enhance metal-catalyzed reactions.

■ ASSOCIATED CONTENT

Supporting Information

The Supporting Information is available free of charge on the ACS Publications website at DOI: 10.1021/acsami.7b08665.

Adsorption energies, reaction pathways, geometries along the reaction pathways, and differential charge density (PDF)

■ AUTHOR INFORMATION

Corresponding Author

*Phone: +86-591-22865872. E-mail: slin@fzu.edu.cn.

ORCID

Sen Lin: 0000-0002-2288-5415

Notes

The authors declare no competing financial interest.

■ ACKNOWLEDGMENTS

We acknowledge support from National Natural Science Foundation of China (21673040) and Natural Science Foundation of Fujian Province (2016J01052).

■ REFERENCES

(1) Qiao, B.; Wang, A.; Yang, X.; Allard, L. F.; Jiang, Z.; Cui, Y.; Liu, J.; Li, J.; Zhang, T. Single-Atom Catalysis of CO Oxidation Using Pt1/FeOx. *Nat. Chem.* **2011**, *3*, 634−641.

(2) Zhao, M.; Yuan, K.; Wang, Y.; Li, G.; Guo, J.; Gu, L.; Hu, W.; Zhao, H.; Tang, Z. Metal-Organic Frameworks as Selectivity Regulators for Hydrogenation Reactions. *Nature* **2016**, *539*, 76−80.

(3) Yuan, B.; Pan, Y.; Li, Y.; Yin, B.; Jiang, H. A Highly Active Heterogeneous Palladium Catalyst for the Suzuki-Miyaura and Ullmann Coupling Reactions of Aryl Chlorides in Aqueous Media. *Angew. Chem.* **2010**, *122*, 4148−4152.

(4) Nasalevich, M. A.; van der Veen, M.; Kapteijn, F.; Gascon, J. Metal−Organic Frameworks as Heterogeneous Photocatalysts: Advantages and Challenges. *CrystEngComm* **2014**, *16*, 4919−4926.

(5) Sutter, P.; Sadowski, J. T.; Sutter, E. A. Sutter. Chemistry under Cover: Tuning Metal- Graphene Interaction by Reactive Intercalation. *J. Am. Chem. Soc.* **2010**, *132*, 8175−8179.

(6) Yao, Y.; Fu, Q.; Zhang, Y. Y.; Weng, X.; Li, H.; Chen, M.; Jin, L.; Dong, A.; Mu, R.; Jiang, P.; Liu, L.; Bluhm, H.; Liu, Z.; Zhang, S. B.; Bao, X. Graphene Cover-Promoted Metal-Catalyzed Reactions. *Proc. Natl. Acad. Sci. U. S. A.* **2014**, *111*, 17023−17028.

(7) Grånäs, E.; Knudsen, J.; Schröder, U. A.; Gerber, T.; Busse, C.; Arman, M. A.; Schulte, K.; Andersen, J. N.; Michely, T. Oxygen Intercalation under Graphene on Ir (111): Energetics, Kinetics, and the Role of Graphene Edges. *ACS Nano* **2012**, *6*, 9951−9963.

(8) Mu, R.; Fu, Q.; Jin, L.; Yu, L.; Fang, G.; Tan, D.; Bao, X. Visualizing Chemical Reactions Confined under Graphene. *Angew. Chem., Int. Ed.* **2012**, *51*, 4856−4859.

(9) Jin, L.; Fu, Q.; Dong, A.; Ning, Y.; Wang, Z.; Bluhm, H.; Bao, X. Surface Chemistry of CO on Ru(0001) under the Confinement of Graphene Cover. *J. Phys. Chem. C* **2014**, *118*, 12391−12398.

(10) Grånäs, E.; Andersen, M.; Arman, M. A.; Gerber, T.; Hammer, B.; Schnadt, J.; Andersen, J. N.; Michely, T.; Knudsen, J. CO Intercalation of Graphene on Ir(111) in the Millibar Regime. *J. Phys. Chem. C* **2013**, *117*, 16438−16447.

(11) Fu, Q.; Bao, X. Surface Chemistry and Catalysis Confined under Two-Dimensional Materials. *Chem. Soc. Rev.* **2017**, *46*, 1842−1874.

(12) Yang, Y.; Fu, Q.; Li, H.; Wei, M.; Xiao, J.; Wei, W.; Bao, X. Creating a Nanospace under an h-BN Cover for Adlayer Growth on Nickel(111). *ACS Nano* **2015**, *9*, 11589−11598.

(13) Zhou, Y.; Chen, W.; Cui, P.; Zeng, J.; Lin, Z.; Kaxiras, E.; Zhang, Z. Enhancing the Hydrogen Activation Reactivity of Nonprecious Metal Substrates via Confined Catalysis Underneath Graphene. *Nano Lett.* **2016**, *16*, 6058−6063.

(14) Fu, Q.; Bao, X. Catalysis on a Metal Surface with a Graphitic Cover. *Chin. J. Catal.* **2015**, *36*, 517−519.

(15) Dong, A.; Fu, Q.; Wei, M.; Liu, Y.; Ning, Y.; Yang, F.; Bluhm, H.; Bao, X. Facile Oxygen Intercalation between Full Layer Graphene and Ru(0001) under Ambient Conditions. *Surf. Sci.* **2015**, *634*, 37−43.

(16) Ma, L.; Zeng, X. C.; Wang, J. Oxygen Intercalation of Graphene on Transition Metal Substrate: An Edge-Limited Mechanism. *J. Phys. Chem. Lett.* **2015**, *6*, 4099−4105.

(17) Blume, R.; Kidambi, P. R.; Bayer, B. C.; Weatherup, R. S.; Wang, Z. J.; Weinberg, G.; Willinger, M. G.; Greiner, M.; Hofmann, S.; Knop-Gericke, A.; Schlogl, R. The Influence of Intercalated Oxygen on the Properties of Graphene on Polycrystalline Cu under Various Environmental Conditions. *Phys. Chem. Chem. Phys.* **2014**, *16*, 25989−6003.

(18) Zhang, Y.; Weng, X.; Li, H.; Li, H.; Wei, M.; Xiao, J.; Liu, Z.; Chen, M.; Fu, Q.; Bao, X. Hexagonal Boron Nitride Cover on Pt(111): A New Route to Tune Molecule-Metal Interaction and Metal-Catalyzed Reactions. *Nano Lett.* **2015**, *15*, 3616−3623.

(19) Ferrighi, L.; Datteo, M.; Fazio, G.; Di Valentin, C. Catalysis under Cover: Enhanced Reactivity at the Interface between (Doped) Graphene and Anatase TiO_2. *J. Am. Chem. Soc.* **2016**, *138*, 7365−7376.

(20) Wang, X.; Chen, X.; Thomas, A.; Fu, X.; Antonietti, M. Metal-Containing Carbon Nitride Compounds: A New Functional Organic-Metal Hybrid Material. *Adv. Mater.* **2009**, *21*, 1609−1612.

(21) Wang, X.; Maeda, K.; Chen, X.; Takanabe, K.; Domen, K.; Hou, Y.; Fu, X.; Antonietti, M. Polymer Semiconductors for Artificial Photosynthesis: Hydrogen Evolution by Mesoporous Graphitic Carbon Nitride with Visible Light. *J. Am. Chem. Soc.* **2009**, *131*, 1680−1681.

(22) Zhang, J.; Chen, X.; Takanabe, K.; Maeda, K.; Domen, K.; Epping, J. D.; Fu, X.; Antonietti, M.; Wang, X. Synthesis of a Carbon Nitride Structure for Visible-Light Catalysis by Copolymerization. *Angew. Chem., Int. Ed.* **2010**, *49*, 441−444.

(23) Wang, Y.; Wang, X.; Antonietti, M. Polymeric Graphitic Carbon Nitride as a Heterogeneous Organocatalyst: From Photochemistry to Multipurpose Catalysis to Sustainable Chemistry. *Angew. Chem., Int. Ed.* **2012**, *51*, 68−89.

(24) Wang, X.; Maeda, K.; Thomas, A.; Takanabe, K.; Xin, G.; Carlsson, J. M.; Domen, K.; Antonietti, M. A Metal-Free Polymeric Photocatalyst for Hydrogen Production from Water under Visible Light. *Nat. Mater.* **2009**, *8*, 76−80.

(25) Chen, X.; Zhang, J.; Fu, X.; Antonietti, M.; Wang, X. Fe-g-C_3N_4-Catalyzed Oxidation of Benzene to Phenol Using Hydrogen Peroxide and Visible Light. *J. Am. Chem. Soc.* **2009**, *131*, 11658−11659.

(26) Kresse, G.; Hafner, J. Ab Initio Molecular-Dynamics Simulation of the Liquid-Metal-Amorphous-Semiconductor Transition in Germanium. *Phys. Rev. B: Condens. Matter Mater. Phys.* **1994**, *49*, 14251.

(27) Kresse, G.; Hafner, J. Ab Initio Molecular Dynamics for Liquid Metals. *Phys. Rev. B: Condens. Matter Mater. Phys.* **1993**, *47*, 558−561.

(28) Kresse, G.; Hafner, J. Ab Initio Molecular Dynamics for Open-Shell Transition Metals. *Phys. Rev. B: Condens. Matter Mater. Phys.* **1993**, *48*, 13115−13118.

(29) Klimes, J.; Bowler, D. R.; Michaelides, A. Chemical Accuracy for the Van Der Waals Density Functional. *J. Phys.: Condens. Matter* **2010**, *22*, 022201.

(30) Dion, M.; Rydberg, H.; Schroder, E.; Langreth, D. C.; Lundqvist, B. I. Van Der Waals Density Functional for General Geometries. *Phys. Rev. Lett.* **2004**, *92*, 246401.

(31) Vydrov, O. A.; Van Voorhis, T. Nonlocal Van Der Waals Density Functional Made Simple. *Phys. Rev. Lett.* **2009**, *103*, 063004.

(32) Kresse, G.; Joubert, D. P. From Ultrasoft Pseudopotentials to the Projector Augmented-Wave Method. *Phys. Rev. B: Condens. Matter Mater. Phys.* **1999**, *59*, 1758−1775.

(33) Bojdys, M. J.; Muller, J. O.; Antonietti, M.; Thomas, A. Ionothermal Synthesis of Crystalline, Condensed, Graphitic Carbon Nitride. *Chem. - Eur. J.* **2008**, *14*, 8177−8182.

(34) Deifallah, F.; McMillan, P. F.; Cora, F. Electronic and Structural Properties of Two-Dimensional Carbon Nitride Graphenes. *J. Phys. Chem. A* **2008**, *112*, 5447−5453.

(35) Aspera, S. M.; David, M.; Kasai, H. First-Principles Study of the Adsorption of Water on Tri-s-triazine-based Graphitic Carbon Nitride. *Jpn. J. Appl. Phys.* **2010**, *49*, 115703.
(36) Lin, S.; Ye, X. X.; Gao, X. M.; Huang, J. Mechanistic insight into the water photooxidation on pure and sulfur-doped g-C_3N_4 photocatalysts from DFT calculations with dispersion corrections. *J. Mol. Catal. A: Chem.* **2015**, *406*, 137−144.
(37) Monkhorst, H. J.; Pack, J. D. Special Points for Brillouin-Zone Integrations. *Phys. Rev. B* **1976**, *13*, 5188−5192.
(38) Blochl, P. E.; Jepsen, O.; Andersen, O. K. Improved Tetrahedron Method for Brillouin-Zone Integrations. *Phys. Rev. B: Condens. Matter Mater. Phys.* **1994**, *49*, 16223.
(39) Chow, H. C.; Vosko, S. H. Special Points for Two-Dimensional Brillouin Zone or Wigner−Seitz Cell Integrations. *Can. J. Phys.* **1980**, *58*, 497−503.
(40) Makov, G.; Shah, R.; Payne, M. C. Periodic Boundary Conditions in Ab Initio Calculations. II. Brillouin-Zone Sampling for Aperiodic Systems. *Phys. Rev. B: Condens. Matter Mater. Phys.* **1996**, *53*, 15513−15517.
(41) Henkelman, G.; Uberuaga, B. P.; Jónsson, H. A Climbing Image Nudged Elastic Band Method for Finding Saddle Points and Minimum Energy Paths. *J. Chem. Phys.* **2000**, *113*, 9901−9904.
(42) Trygubenko, S. A.; Wales, D. J. A Doubly Nudged Elastic Band Method for Finding Transition States. *J. Chem. Phys.* **2004**, *120*, 2082−2094.
(43) Peters, B.; Heyden, A.; Bell, A. T.; Chakraborty, A. A Growing String Method for Determining Transition States: Comparison to the Nudged Elastic Band and String Methods. *J. Chem. Phys.* **2004**, *120*, 7877−7886.
(44) Henkelman, G.; Arnaldsson, A.; Jonsson, H. A Fast and Robust Algorithm for Bader Decomposition of Charge Density. *Comput. Mater. Sci.* **2006**, *36*, 354−360.
(45) Ma, Z.; Zhao, X.; Tang, Q.; Zhou, Z. Computational Prediction of Experimentally Possible g-C_3N_3 Monolayer as Hydrogen Purification Membrane. *Int. J. Hydrogen Energy* **2014**, *39*, 5037−5042.
(46) Larciprete, R.; Ulstrup, S.; Lacovig, P.; Dalmiglio, M.; Bianchi, M.; Mazzola, F.; Hornekær, L.; Orlando, F.; Baraldi, A.; Hofmann, P.; Lizzit, S. Oxygen Switching of the Epitaxial Graphene-Metal Interaction. *ACS Nano* **2012**, *6*, 9551−9558.
(47) Lin, S.; Huang, J.; Gao, X. A Cu(111) Supported h-BN Nanosheet: A Potential Low-Cost and High-Performance Catalyst for CO Oxidation. *Phys. Chem. Chem. Phys.* **2015**, *17*, 22097−22105.

DOI: 10.1021/acsami.7b08665
ACS Appl. Mater. Interfaces 2017, 9, 33267−33273